

Intercalibration of the reflective solar bands of MODIS and MISR instruments on the Terra platform

Amit Angal,^{a*} Carol Bruegge,^b Xiaoxiong Xiong,^c Aisheng Wu^a

^a Science Systems and Applications Inc., 10210 Greenbelt Road, Lanham, MD 20706

^bNASA, Jet Propulsion Laboratory, California Institute of Technology, Pasadena, CA 91109, USA

^c Sciences and Exploration Directorate, NASA GSFC, Greenbelt, MD 20771

Abstract. As a part of NASA's Earth Observing System (EOS), the Terra spacecraft was launched on December 18, 1999, with the goal of understanding the changes of the Earth, by examining the Earth's hydrological, geophysical, and climatic processes. The MODIS and MISR instruments on the Terra platform, combined with their continuous operation, broad spectral coverage, and different spatial resolutions, have played an important role to achieve the goals of the EOS. Over two decades of successful operations, these multispectral imaging instruments have benefited a variety of scientific applications. Being on the same platform, the two sensors complement each other in terms of spatial coverage (and target viewing geometry) and facilitate synergistic applications using multispectral data. A consistent radiometric calibration between these sensors is a prerequisite for creating high quality science products from their observations. Both instruments underwent intensive prelaunch characterization and their on-orbit calibrations are monitored using their onboard calibrators. In this paper, we perform a calibration inter-comparison of the spectrally matching bands of the two instruments using vicarious techniques. These techniques include multiyear simultaneous views of the North African desert, North Atlantic Ocean, and Dome Concordia, therefore covering different reflectance regimes. Also included in this work are the near-simultaneous top-of-atmosphere (TOA) reflectance measurements from Railroad Valley, USA, as provided by the RadCalNet (converted to TOA), that are used as a calibration reference to compare the on-orbit observations between MODIS and MISR. Simultaneous overpasses from desert, ocean, Dome C, and RadCalNet over Railroad Valley reveal that the agreement between the four spectrally matching bands is within 3% for the time-period between 2014 and 2020. Also, observed are some long-term drifts in the TOA reflectance time-series from MISR for the red and NIR band that are expected to be corrected in a future calibration reprocess.

Keywords: MODIS, Terra, MODIS, MISR, cross-calibration

*First Author, E-mail: amit.angal@ssaihq.com

1 Introduction

With a payload of five remote sensing instruments, Terra spacecraft was successfully launched on December 18, 1999, from Vandenberg Airforce Base, California, USA. Two key instruments on the Terra spacecraft, the Moderate Resolution Imaging Spectroradiometer (MODIS) and Multi-angle Imaging Spectroradiometer (MISR) facilitate a wide variety of scientific applications in the reflective solar region. Raytheon Santa Barbara Remote Sensing (SBRS), Goleta, CA, developed the MODIS instrument and performed extensive preflight characterization and calibration measurements.¹⁻² MISR was designed and built by the Jet Propulsion Laboratory (JPL), Pasadena,

CA and underwent its own extensive prelaunch characterization. Both instruments met the design requirements and have continued the excellent performance on-orbit and provided two decades of high-quality scientific measurements. In addition to intensive prelaunch characterization, both instruments are regularly calibrated on-orbit using a combination of solar, lunar (only MODIS for long-term stability), and vicarious measurements.³⁻⁵ Several scientific applications and products involve a synergy of measurements from these two instruments therefore highlighting the need for a consistent and accurate data record. The longevity of operations, aging instruments, and degrading performance have led to challenges in achieving a consistent data record. In this paper, we utilize the advantages of simultaneous Earth view imaging by MODIS and MISR to perform a cross-calibration between the spectrally matching bands using vicarious calibration techniques.

Simultaneous nadir-viewing scenes from the two instruments over the North African desert, North Atlantic Ocean, and Dome Concordia in Antarctica are chosen for this work. A set of common geolocation points, identified over a defined region of interest, are used to compute the at-sensor reflectance and other statistics. Additional corrections for spectral response function mismatches are also applied. In addition to the three sites, an additional instrumented site is also chosen for this comparison. The RadCalNet, a Committee on Earth Observation Satellites (CEOS) initiative, has provided SI-traceable TOA reflectances from a network of instrumented land-based sites.⁶ One such site is the Railroad Valley Playa, Nevada (RRV) which is a high altitude, dry lakebed. The RadCalNet provides an at-sensor hyperspectral reflectance profile based on the measurements from its ground viewing radiometers.⁶ Together with the direct views of RRV by MODIS and MISR, the RadCalNet provided measurements facilitate developing the necessary corrections to account for spectral response function mismatches.

The spectrally matching land-viewing bands of MODIS and MISR are seen to generally agree to within 3% over desert, Dome C and RRV, with a greater bias observed for the red and near-infrared band pairs while viewing the low radiance ocean scenes. Also included in this paper is a description of various uncertainties associated with this cross-calibration over these targets. During the prelaunch characterization of the Terra MODIS instrument, some short wavelength bands were identified to be particularly sensitive to the polarization of the incident light, with on-orbit results further reaffirming that the polarization sensitivity has experienced changes that are wavelength, mirror side and scan angle dependent.⁷ A brief discussion of the MODIS polarization impact on the blue band cross-calibration is also included. MISR polarization insensitive due to the inclusion of a Lyot depolarizer as the front element of each camera.

Finally, the Terra spacecraft is expected to exit the AM constellation in the coming years which bears some impacts on the quality of the Level 1B data produced by the MODIS and MISR instruments. A brief discussion about the impacts of this event on the cross-calibration between these instruments is also discussed in this paper.

2 Methodology

2.1 Reflectance data products

Top-of-atmosphere reflectance, ρ_{toa} , is a measure of the at-sensor radiance, L , scaled by the exo-atmospheric irradiance, E_0 . Specifically,

$$\rho_{toa} = \pi L d^2 / E_0$$

where d the Earth-Sun distance. While MODIS can directly measure the incident solar irradiance, using the Solar Diffuser Stability Monitor (SDSM), ρ_{toa} is the more accurate data product. To

derive radiance, the MODIS L1B data product makes use of a solar irradiance spectrum which is a compilation of solar models by Thuillier et al., (1998) from 0.4 μm to 0.8 μm , Neckel and Labs (1984) from 0.8 μm to 1.1 μm , and Smith and Gottlieb (1974) above 1.1 μm .⁹⁻¹¹

MISR established its radiometric scale, early in the mission, on vicarious calibration experiments using surface reflectance measurements, a radiative transfer code, and the Wehrli exo-atmospheric solar spectrum model. In-flight calibration then maintains radiometric accuracy by using on-board-calibrator and desert-site trend studies. As MISR and MODIS use different solar models, a comparison of TOA radiances would have an additional bias, related to the difference in these two solar models. As shown in Bruegge et al. (2021), this is a 3% bias in the blue band, and negligible for the other three bands.¹²

2.2 Sensor Overview

MODIS has 36 spectral bands located on four focal plane assemblies with wavelengths ranging from 0.4 to 14.4 μm and spatial resolutions of 250 m (Bands 1 and 2), 500 m (Bands 3 to 7), and 1000 m (Bands 8 to 36). Its reflective solar bands (Bands 1-19 and 26) from 0.41 to 2.1 μm are calibrated on-orbit by a solar diffuser (SD) and the thermal emissive bands (Bands 20-25, 27-36) from 3.75 μm to 14.2 μm are calibrated using a blackbody. Using a rotating double-sided paddle wheel scan mirror scanning over a range of -55° to $+55^\circ$ from instrument nadir, MODIS provides a 10 km (nadir) along track by 2330 km cross-track swath each scan.² The SD, together with the SDSM, provide a reflectance-based on-orbit calibration for the MODIS reflective solar bands (RSB). In addition to the solar observations, measurements from the Moon as well as response trending from the desert sites are used to characterize the on-orbit change of the scan-angle dependence, commonly referred to as response versus scan angle (RVS). The on-orbit performance of the MODIS RSB continues to be stable and largely compliant with the 2% uncertainty

requirement (in reflectance) with a few exceptions. Recent publications from Xiong et al. 2019, summarize the on-orbit performance of the MODIS RSB in detail.¹³⁻¹⁴

A unique feature of the MISR instrument is the nine cameras pointed at fixed angles, one viewing the nadir and four each viewing the fore and aft directions along the spacecraft ground track, providing measurements across many scattering angles. MISR can acquire imagery at two different spatial resolution modes. In the local mode, select targets are observed at 275 m spatial resolution with all cameras and wavelengths. However, due to the limitations with the data transmission rates, in the global mode operation the resolution in the off-nadir cameras is reduced to 1.1 km in instrument's three spectral bands (the red band resolution is retained at 275 m). Data from the nadir camera is always reported at the higher resolution. In this work, we only consider the results from the nadir (An) camera. MISR employs regular on-board calibration to track the radiometric response changes. On an approximately bi-monthly basis, Spectralon panels are deployed to reflect sunlight into reference photodiode detectors and the MISR CCD cameras simultaneously to compute the gain coefficients for each of the 1504 pixels. A key difference between the two instruments is the fact that MISR acquires data in a pushbroom manner using the CCD cameras whereas MODIS acquires it in a whiskbroom manner using a scan mirror. The MISR on-orbit performance is summarized in detail by Bruegge et al. (2002).⁵ The key characteristics of the MODIS and MISR instruments pertaining to this intercalibration are summarized in Table I.

The four spectrally matching bands chosen for this work are also summarized in Table I. Among the chosen MODIS bands, Band 9 is a high-gain band designed for ocean applications and is therefore prone to saturation over high radiance targets such as Dome C. In addition to bands listed here, there are other MODIS ocean bands that also spectrally overlap with MISR red and NIR bands but are not considered here as they are affected by saturation.

Table 1 Summary of key characteristics of the MODIS and MISR RSB

	MODIS	MISR
Swath	2330 km	380 km
Spatial Resolution (at nadir)	250 m, 500 m, 1km	275 m
Spectral Coverage	Band 9 (0.442 μm)	Blue (0.446 μm)
Band (Center Wavelength)	Band 4 (0.555 μm)	Green (0.558 μm)
	Band 1 (0.645 μm)	Red (0.672 μm)
	Band 2 (0.858 μm)	NIR (0.867 μm)

2.3 Data Reduction

Being on the same spacecraft, continuous simultaneous observations of the Earth's surface at nadir are acquired by the MODIS and MISR RSB. Therefore, the intercalibration between the two instruments can be performed using any given target on the Earth. While a scene-independent approach can provide a reliable long-term stability assessment of the reflectance ratios between the two instruments, applying a correction for the spectral response mismatch can be challenging without prior knowledge of the spectral signature of the incident light. To overcome this limitation, three ground targets, North African (Saharan) desert, North Atlantic Ocean and Dome Concordia that have a known spectral signature are chosen for this study. Each MISR L1B2 Ellipsoid product covers an entire orbit and is subdivided into 180 equally sized blocks. A fixed number of blocks are selected from every overpass of these sites over the mission lifetime and the details are summarized in Table II. The MODIS L1B Collection 6.1 granules were obtained from the LAADS (<https://ladsweb.nascom.nasa.gov/>). The MISR data sets (version F03_0024) were obtained from the NASA Langley Research Center Atmospheric Science Data Center.

Table 2. MISR Path and Block selection

Site	North African desert	North Atlantic Ocean	Dome C
Path, Blocks	179, 75-80	223, 65-70	089, 150-153

The MODIS L1B granules cover a 5-minute interval with swath of 2330 km (cross track) x 2030 km (along track at nadir). The MISR geolocation is provided at 1.1 km resolution and MISR's nadir 275 m data is averaged to 1.1 km to match with the MODIS 1km resolution. To retrieve the MODIS geolocated pixels at 1 km resolution, the MODIS L1A geolocation product (MOD03) is used to extract a per-pixel latitude and longitude values. The distance between a MODIS and a MISR pixel is computed based on these latitude and longitude values and pixel pairs with distance less than 250 m are retained for subsequent processing. Typically, about 20,000 co-located pixels are retained for each overpass over the North African desert and North Atlantic Ocean, each consisting of 6 MISR blocks. The TOA reflectance from these co-located pixels is computed for both instruments on a per-band basis. In the case of MODIS, additional information, such as mirror side, frame (scan angle) and detector, is also retained. This information has previously been used to monitor the MODIS RSB detector and mirror side differences and is summarized in detail in Angal et al., 2018.¹⁵ Finally, a reflectance ratio for each spectrally matching band is computed and an average of all the ratios for a given event are computed.

Using the spectral-band adjustment factor (SBAF) tool developed by NASA Langley, a correction for relative spectral response mismatch is applied based on representative hyperspectral reflectance profiles from SCIAMACHY observations. The correction factors used in this study are site and band-dependent, but are time-independent, primarily due to unavailability of simultaneous SCIAMACHY hyperspectral observations. The SCIAMACHY correction factors were derived from clear-sky observations over PICS and all-sky observations over Dome C and ocean targets. The clear-sky conditions were determined by applying a spatial homogeneity threshold to a standard deviation of the visible channel reflectance.¹⁶ In this analysis, we used a spatial

homogeneity threshold to a standard deviation; however, since the MODIS and MISR are viewing simultaneously, the impacts were found to be minimal.

In addition to the three sites chosen above, an additional instrumented site is also chosen. The RadCalNet, a CEOS initiative, has provided SI-traceable TOA reflectances from a network of instrumented land-based sites located in LaCrau, France, Gobabeb in Namibia, and Baotou in China, in addition to RRV. Among the four sites, the RRV has the most coincident measurements and subsequently at-sensor predicted TOA reflectances that can be used as reference to compare MODIS and MISR. Automated measurements, including surface reflectance and other atmospheric measurements are available, from the RadCalNet portal, every 30 minutes between 09:00 and 15:00 local time and post-processed products include TOA reflectance at nadir between 0.4 to 2.5 μm , after radiative transfer calculations. The MODIS and MISR overpass, obtained once every 16 days, at around 10:30 am local standard time is used to extract the TOA reflectance on a 1km x 1km area surrounding the ground viewing radiometers. The RadCalNet reflectances are band-weighted by the MODIS and MISR Relative Spectral Response (RSR) to derive an at-sensor predicted TOA reflectance that is used to normalize the measured TOA reflectance, effectively cancelling out the spectral differences and atmospheric variations on the MODIS/MISR reflectance ratios. A total of 147 simultaneous overpasses between MODIS and MISR over RRV were processed from January 1, 2013 to January 1, 2021. These were further reduced to 57 after excluding the overpasses that did not have corresponding Radcalnet data. As these are simultaneous views of the site, no further filtering for potentially cloudy or partially cloudy scenes is applied.

Figure 1a shows the TOA and surface reflectance profile over RRV site from September 28, 2020 (sampled at 18:30 UTC) plotted along with the MODIS and MISR RSRs. A difference of about 5-

6% between the TOA and surface reflectance is observed between the red band range and less than 1% difference in the NIR range. For every measurement, the band-integrated RadcalNet TOA reflectance for each MODIS and MISR band is used to compute the RadcalNet predicted TOA reflectance. In Figure 1b, the TOA reflectance ratio from the RadcalNet predicted reflectances for the spectrally matching MODIS and MISR bands is plotted. These ratios represent the differences in the TOA reflectance over RRV caused due to the RSR mismatch between the two sensors. Apart from the red bands (MODIS band 1 and MISR red), the observed agreement is within 2%. with no apparent temporal drift over the 7 years of available data series. It can also be seen that there is no significant long-term trend or drift from the RadcalNet provided TOA reflectances.

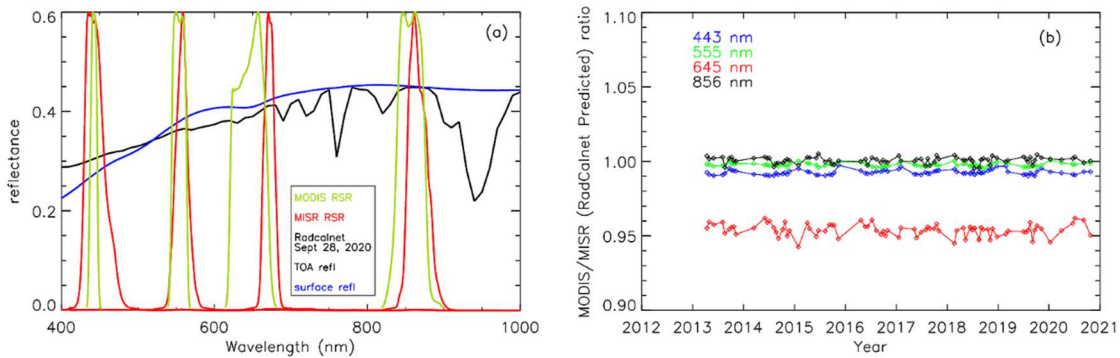


Fig. 1 (a). MODIS and MISR RSR plotted over a sample RRV Radcalnet profile (b) Radcalnet predicted TOA reflectance ratios

3 Results and Discussions

In this section, the results from all the four targets are presented and discussed.

3.1 Ground Sites results

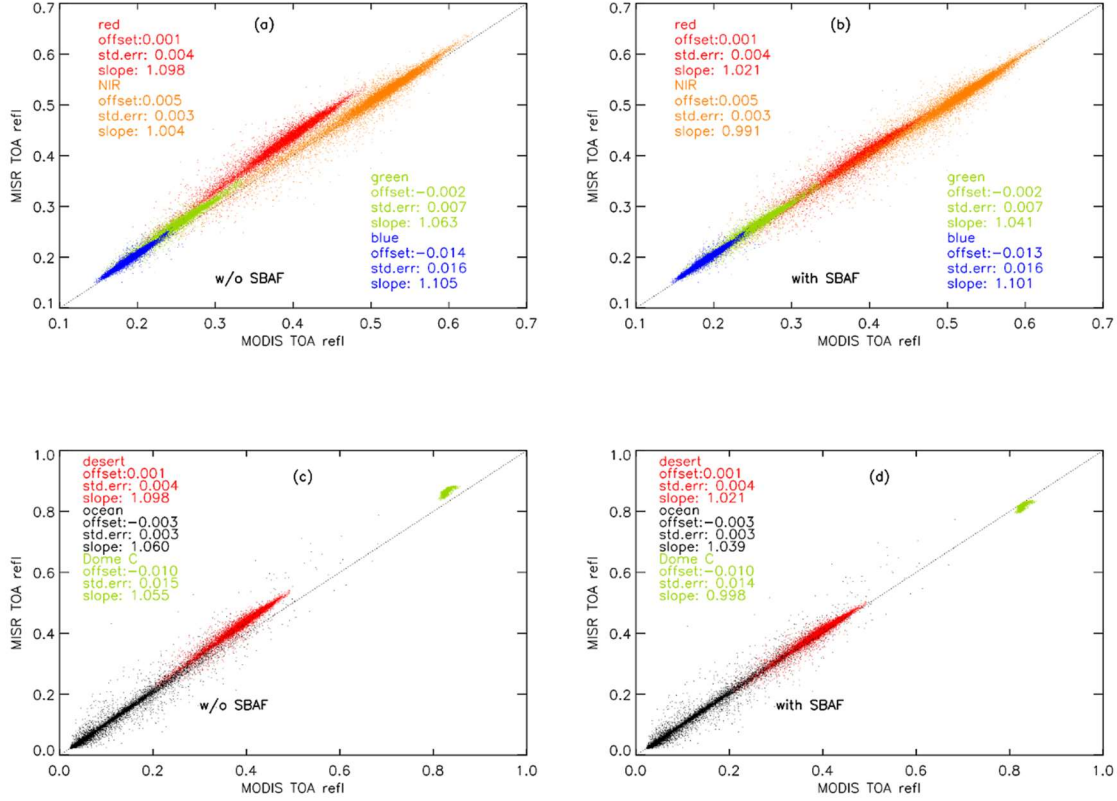


Fig. 2(a). MODIS-MISR TOA reflectance regression for a North African desert overpass from February 2020 without SBAF correction (b) with SBAF correction. (c) MODIS-MISR TOA reflectance regression for the three ground sites using scene pairs from February 2020 for the red-band pair without SBAF correction. (d) with SBAF correction

Over the desert, ocean, and Dome C sites, a nadir overpass of MODIS and the corresponding MISR pair is selected at a frequency of once every 16 days. The results from one such overpass pair is plotted in Figure 2a where the TOA reflectances from geo-matched pixels for the spectrally matching MODIS and MISR bands are plotted against each other with a dotted line showing one-to-one values. From the figure above, no obvious non-linear behavior is observed in any of the band-pairs. The offset in the trends from the one-to-one line is predominantly due to the spectral band-pass differences between the two instruments. In Figure 2c., a similar plot for the red-band

pair is plotted using an overpass over three sites, ocean, desert, and Dome C. As expected, the reflectance levels from the three targets cover a large part of the dynamic range, with the Dome C site being the brightest and ocean sites showing the lowest reflectance values as expected. Similar to Figure 1a, no non-linear behavior is observed across the dynamic range, a behavior that is also consistent across the other bands, not shown here. Using a simple linear regression, the offset, slope, and standard error were determined for each case as listed on the plot with small offset values observed in all cases. Figures 2(b) and 2(d) show the results after SBAF correction. In most cases, the slope of the trends post-SBAF correction are closer to unity indicating improvement, while in the remaining cases, a slight overcorrection is observed. This can be attributed to the fact that a SBAF correction is time-independent and might not adequately capture the day to day scene variations.

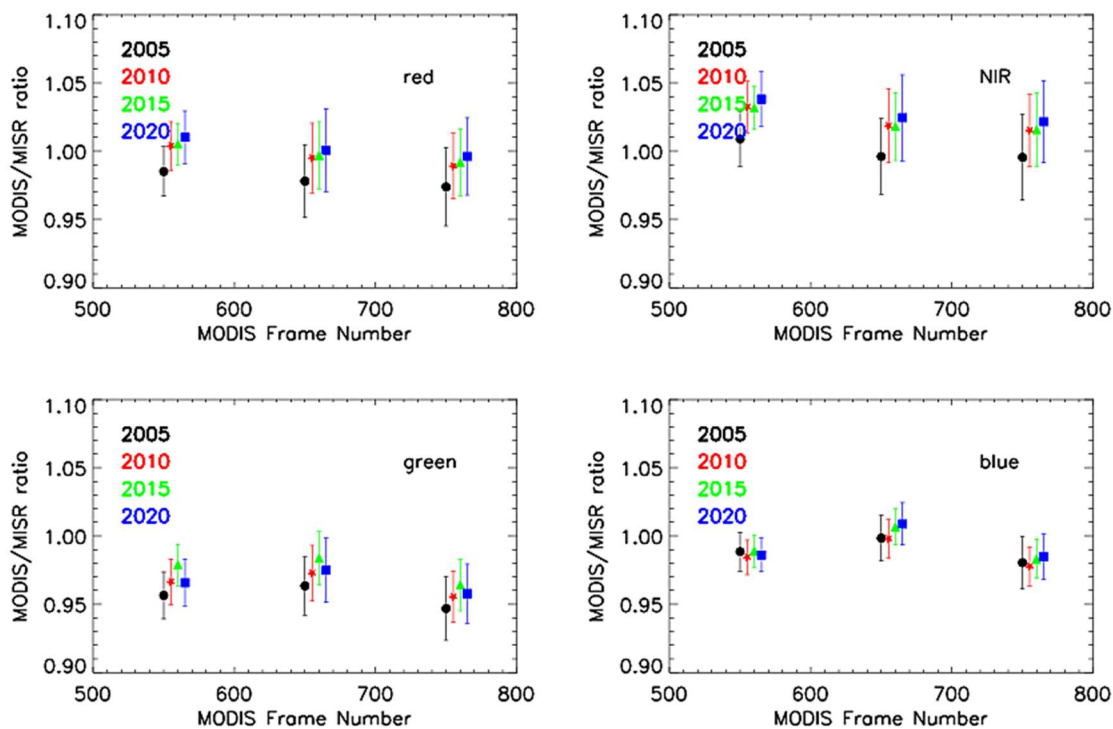


Fig. 3. MODIS/MISR TOA reflectance ratios (SBAF corrected) as a function of MODIS frame number (scan angle) from multiple years (a) blue bands (b) green bands (c) red bands (d) NIR bands.

Unlike MISR, which employs a CCD imaging mechanism, MODIS is a scanning radiometer with the double-sided scan mirror covering a large swath of $\pm 55^\circ$ around nadir, equivalent to 1 to 1354 frames as denoted in MODIS L1B product. The MISR imaging swath overlaps with MODIS at nadir covering the equivalent frame range between 500 and 800. The MODIS RSB calibration formulation has a correction built in for the variation of the response versus scan-angle (RVS) that has shown large changes over the mission at the shortest wavelengths. Figure 3 examines the stability of the MODIS and MISR reflectance ratios over the desert sites after correction using the SBAFs discussed earlier. Four overpass pairs from 2005, 2010, 2015, and 2020 are chosen and the per-pixel reflectance ratios are binned and averaged across three bins of 100 frames, frame 500-600, frame 600-700, and frame 700-800 to compute a mean and 1-sigma across the TOA reflectance ratios. A 1-2 % variation in the reflectance ratios is observed across the frame bins, with most variation observed in the blue band pair. Also seen from this result is a temporal trend in these reflectance ratios particularly for the red and NIR bands.

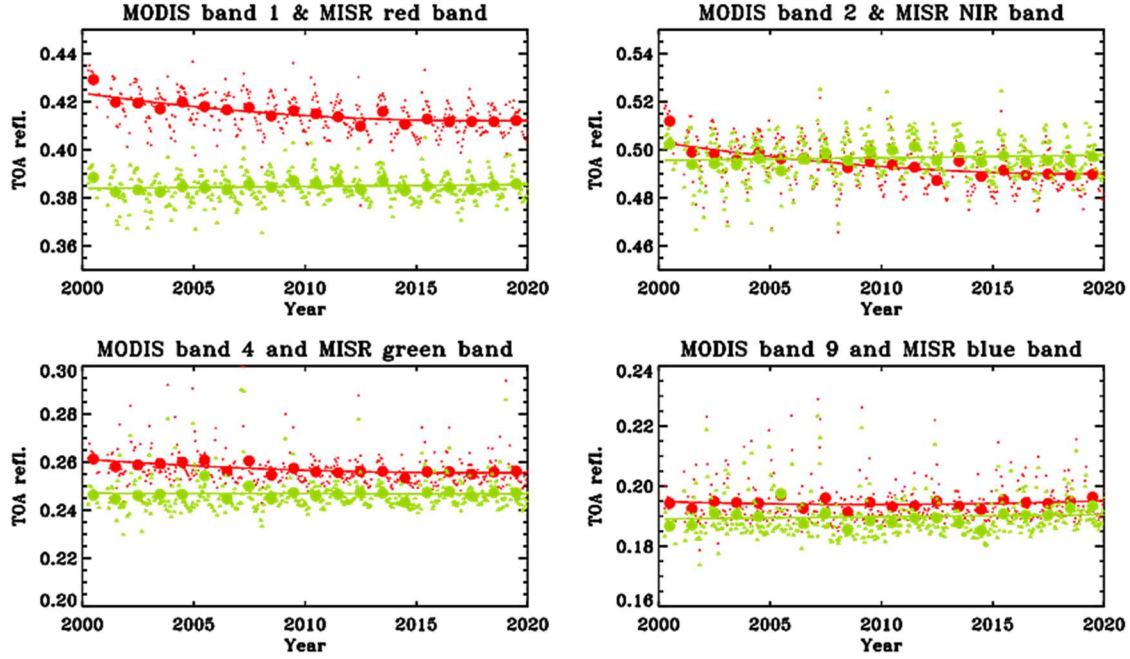


Fig. 4. At-sensor reflectance trending over the North African desert target for the analogous MODIS and MISR bands (plotted in green and red colors, respectively).

Using the methodology described earlier, at-sensor reflectance ratios for the co-located MODIS and MISR pixels is computed. Figure 4 shows the TOA reflectance trends for the spectrally matching MODIS and MISR bands over the North African desert site, with MODIS data shown in green and MISR in red. The yearly-averaged TOA reflectance is shown in circles along with a quadratic exponential model fit to estimate the long-term drift. The seasonal oscillations vary in the individual measurements, an expected behavior attributed to the view-geometry variations. In short wavelength band pair ($0.442 \mu\text{m}$), noticeable variations in the TOA reflectance trends can be seen that are likely due to the Rayleigh scattering. Since these are simultaneous observations, these effects are absent from the at-sensor reflectance ratios, as will be shown in the later results. A multi-year reflectance drift is observed in the red and NIR bands of MISR. This was also earlier noted by Limbacher and Kahn (2017).¹⁷ The trend appears to be more pronounced in the first

decade of operation and levels out after about 2010 and was also reported previously.¹⁸ A detail correction for these temporal drifts has already been developed by the MISR team and is discussed in the next section.

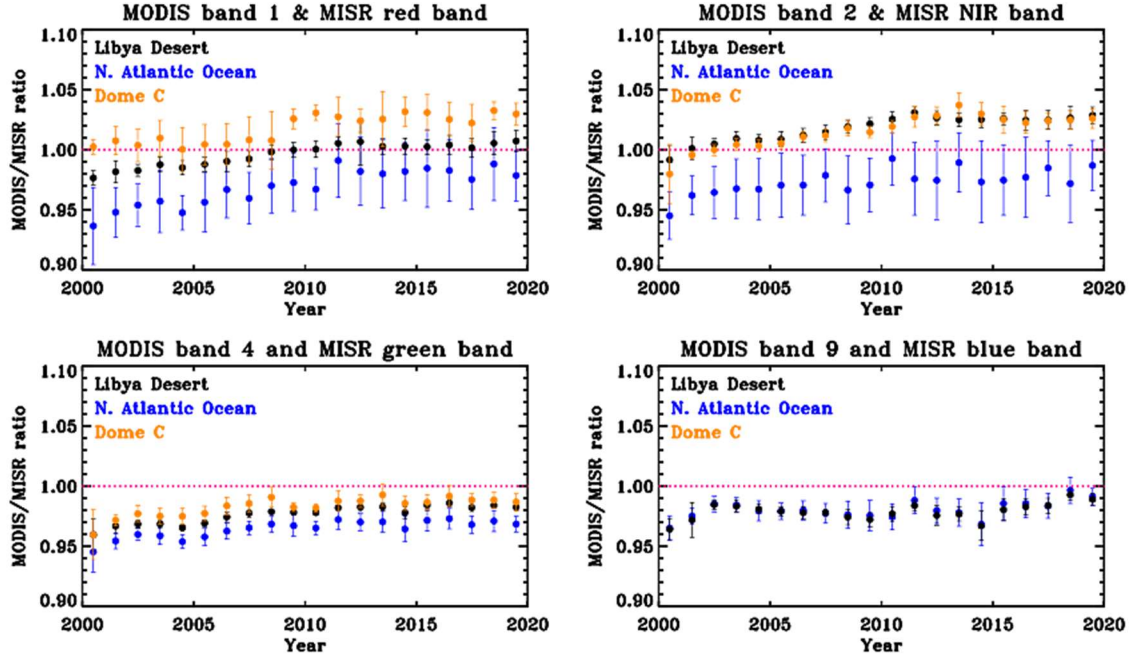


Fig. 5. At-sensor reflectance ratios over multiple targets for the analogous MODIS and MISR bands.

Figure 5 shows the per-year reflectance ratios for the spectrally matching bands including the trends from the three sites chosen for this study. The SBAF correction has already been applied to these results. MODIS Band 9 shows partial saturation when viewing the high radiance Dome C target and hence is not shown. The reflectance drift in the MISR red and NIR bands shown in Figure 4 is reaffirmed in Figure 5 with the results from the desert and Dome C showing up to 2% drift over the two decades of operation. A noticeable disagreement is observed in the MODIS to MISR reflectance ratios from the North Atlantic Ocean site with the ratios vary between 0.99 (1%) to 0.93 (7%) for the red band and between 0.99 (1%) to 0.94 (6%) for the NIR band pair. The

MODIS Bands 1 and 2 are the land viewing bands and as a result retrieve very low signal over the ocean targets. To further investigate this bias, the MODIS to MISR reflectance ratio is also computed using Band 13 (0.65 μm) and Band 16 (0.86 μm) as shown in Fig. 6. Although these bands have a similar center wavelength as Bands 1 and 2, they are high-gain bands designed for ocean color applications and saturate while viewing the desert and Dome C sites. Although MODIS band 16 is indicating a similar trend as MISR NIR band, it should also be noted that any conclusions long-term drift are less reliable due to the higher error bars associated with these trends. The MODIS to MISR reflectance ratios from the North Atlantic Ocean site where the ratios vary between 0.99 (1%) to 0.96 (4%) for the red band and between 0.97 (3%) to 0.95 (5%) for the NIR band pair. The Atlantic Ocean site results are likely influence by the known ghosting and veiling light radiometric artifacts in the MISR cameras, as described by Bruegge et al. (2002, 2014), Limbacher and Kahn (2015), and Witek et al. (2018).^{5,12,19-20} These low-light-level contrast-dependent stray light effects mainly manifest in dark oceanic scenes and in the NIR and red spectral bands, consistent with the results observed in Fig. 6. A simple correction was introduced in MISR Level 2 processing for aerosol retrievals (Witek et al., 2018; Garay et al., 2020), but a more sophisticated stray light correction model will be applied to the MISR L1B2 radiance products in the near future.²⁰⁻²¹ The study of aerosols over ocean is one of the important goals for MISR as well as the MODIS instrument and special attention must be given to this radiometric calibration disagreement to ensure the reliability of the downstream products involving information from both instruments. For this reason, it will be interesting to repeat this cross-comparison exercise with reprocessed MISR data, which will include the ghost-correction algorithm important for ocean scenes.

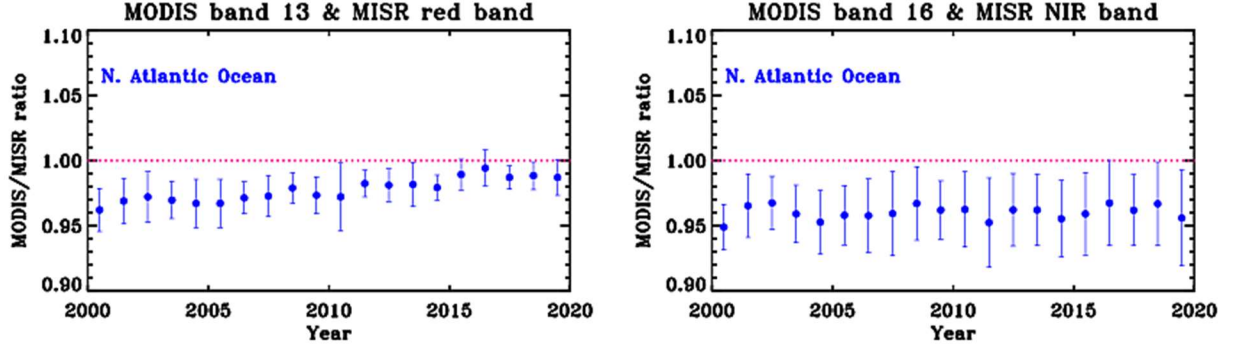


Fig. 6. At-sensor reflectance ratios over North Atlantic Ocean for the analogous MODIS ocean bands and MISR bands.

3.2 RadCalNet-based results

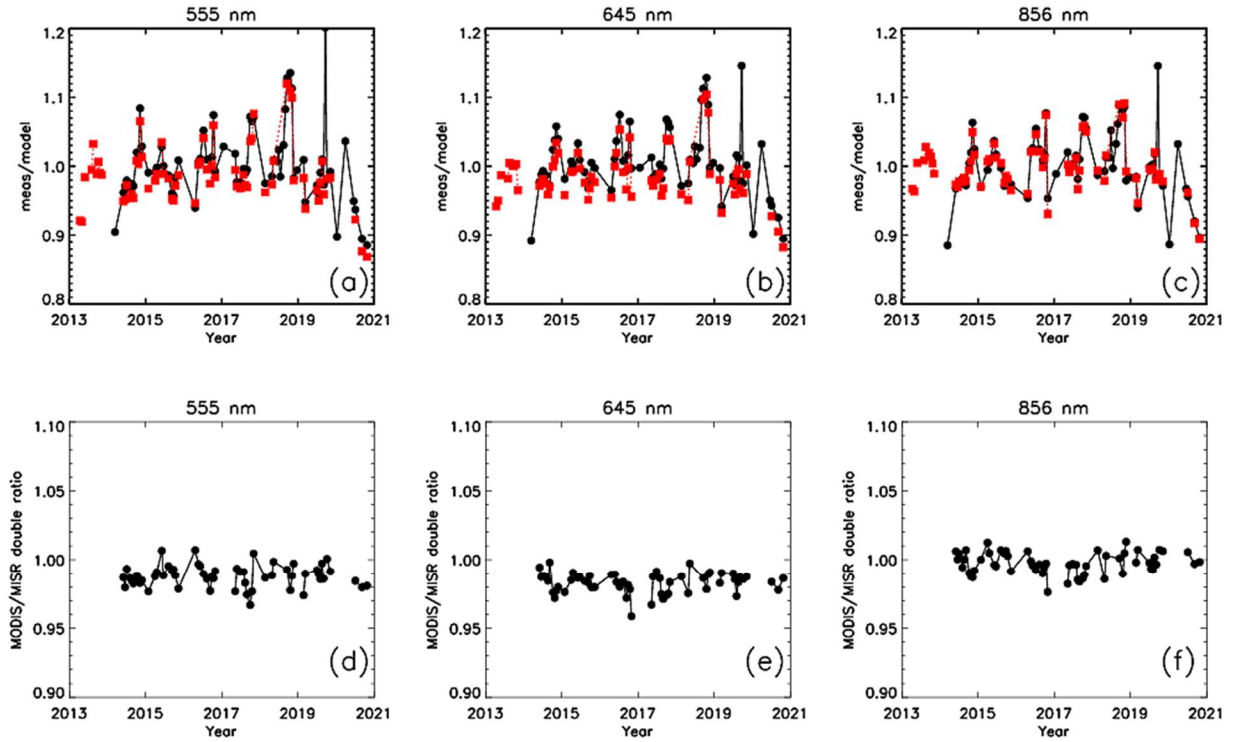


Figure 7 (a) Green, (b) Red, and (c) NIR bands (measured/model of all available RadCalNet matchups). MODIS data is shown in red and MISR in black. Blue band pair not shown here due

to saturation observed in MODIS data. The panels (d)-(f), show the corresponding MODIS/MISR double ratio from the same-day overpasses.

Figure 7. shows the measured TOA reflectances over RRV normalized by the RadCalNet predicted reflectances for the green, red and NIR bands. All the TOA reflectances that have corresponding RadCalNet matchups are shown here. In general, the MODIS TOA reflectance measurements after normalization are seen to be about 1-2% lower than the corresponding MISR measurements. The fluctuations in the time-series of the normalized TOA reflectances of either instrument can be attributed to the uncertainties associated with the RadCalNet TOA reflectances, but the effects of this are significantly diminished when considering the double ratio $(\frac{\rho_{MODIS-TOA}}{\rho_{MODIS-RadCalpredic}})/(\frac{\rho_{MISR-TOA}}{\rho_{MISR-RadCalpredic}})$ also plotted in Figure 7.

Table III provides a summary of the MODIS/MISR ratios from the four different ground targets over a common 6-year period. The results from desert, ocean and Dome C sites are corrected for RSR mismatch using SCIAMACHY observations whereas RadCalNet provides real-time information of the spectral signature of the RRV site that is used to correct the at-sensor reflectance ratios. The results over Dome C and RRV for the 443 nm channel were unavailable due to the saturation of the high-gain MODIS Band 9. The results from multiple sites are seen to agree within $\pm 2\%$ except for the ocean site where 645 nm and 856 nm bands show larger disagreement compared with desert and Dome C, which is likely due to stray light effects in MISR cameras.

Table 3. Summary of MODIS/MISR ratios (2014-2020) over multiple targets

	desert		ocean		Dome C		RadCalNet	
Band	mean	std.dev	mean	std.dev	mean	std.dev	mean	std.dev
645 nm	1.004	0.008	0.982	0.027	1.028	0.013	0.983	0.007
856 nm	1.026	0.007	0.978	0.029	1.027	0.008	0.997	0.008
555 nm	0.983	0.004	0.970	0.008	0.989	0.007	0.988	0.007
443 nm	0.982	0.007	0.983	0.012	N/A	N/A	N/A	N/A

3.3 Discussions

The longevity of the two instruments, MODIS and MISR, make them a benchmark against which on-orbit calibration of the newer instruments is verified. The instruments, with a different radiometric calibration process, are calibrated independently, hence an assessment of the calibrated products, as presented in this study is of paramount importance. Since simultaneous nadir views of the desert, ocean, and Dome C sites are primarily used in this study, the effects due to site and atmosphere bi-directional reflectance distribution factor (BRDF) are expected to have diminished impacts and hence corrections using a semi-empirical or physical BRDF models is not considered. A correction of BRDF effects is essential and is included in the production of the downstream science products (such as surface reflectance) from each instrument. MODIS' specified calibration uncertainty requirements are 2% in reflectance for the RSB at typical scene radiance levels and observations within $\pm 45^\circ$ scan angle range, whereas the MISR absolute uncertainty calibration requirements are 4% for its four bands. As discussed earlier, the blue band for MODIS (Band 9) has experienced significant degradation on-orbit in addition to observed changes in its polarization sensitivity, which has particularly large impacts towards the end of the MODIS scan. Although the impact at nadir is expected to be minimal, the MODIS TOA reflectances over the desert site were corrected using a set of polarization correction coefficients and a methodology described in ²² to confirm that the magnitude of corrections is less than 0.2% for the blue band and less than 0.1% for the other bands. Since both instruments are on the same platform and provide simultaneous imaging, the temporal, spatial, or spectral stability of the ground target has a diminished impact on the multi-year cross calibration.

Table 4. Summary of MODIS and MISR cross-calibration uncertainty sources

Uncertainty Source	Uncertainty (%)
MODIS calibration uncertainty	2%
MISR calibration uncertainty	4%
SBAF uncertainty	0.5-2%
Atmospheric effects	2-3%
Total Uncertainty	4-6%

3.4 Future Efforts

Over the two decades on-orbit operations, multiple upgrades to the MODIS L1B algorithm have resulted in the delivery of well-calibrated scientific data products. While the current MODIS L1B version 6.1 is expected to continue operations, an improved version of the MODIS L1B, version 7, is expected to be in production in early 2022. This new version incorporates several improvements for the MODIS RSB, primarily in the SWIR bands and towards the end of scan for the short wavelength VIS bands. In the case of the bands chosen in this work, the differences between C7 and C6.1 at nadir are expected to be less than 1%.

Similar reprocessing efforts are also underway for the MISR L1B products. Multiple corrections will be introduced that will address some of the issues highlighted in earlier sections and improve the overall radiometric accuracy of MISR observations. A temporal trend correction (Limbacher and Kahn (2017)), using Sahara Desert sites, will address small but noticeable radiometric drifts in all MISR spectral bands and cameras, examples of which are seen in Fig. 4 and Fig. 5. A flat fielding correction will address cross-track artifacts in MISR nadir-viewing camera, especially in the blue and green spectral bands.¹⁷ Furthermore, a ghosting and veiling light correction model—

based on ray-tracing simulations of light propagation within the MISR cameras—will be implemented to eliminate stray light artifacts in high-contrast scenes. This will largely mitigate the MISR/MODIS reflectance ratio disagreements seen in Fig. 5 and Fig. 6 for the North Atlantic Ocean site. Some other radiometric improvements include transitioning to the TSIS-1 solar model (Coddington, et al., 2021) and seasonal smoothing of on-board calibration coefficients.²³ Most of the corrections mentioned above are already in their final stages of development; operational implementation and L1B product reprocessing are anticipated to take place in 2022.

Over the Terra's mission, the regular inclination adjust maneuvers maintained the platform's mean local time (MLT) of its equator crossing (10:30 am). Due to fuel constraints, no IAMs are performed and as a result the Terra MLT has begun drifting and in October, 2022 it is expected to reach and exceed a 10:15 am MLT and a constellation exit maneuver to a lower orbit altitude (694 km) is expected. Additional considerations for changes in the ground sampling distance need to be made to continue the use of this technique for comparing the performance between MODIS and MIS beyond October 2022.

4 Summary

The Terra mission continues to operate successfully providing valuable scientific measurements serving various land, atmosphere, ocean, and cryosphere products. An inter-comparison between the reflective solar bands of the two key instruments on the Terra platform, MODIS and MISR, has been performed in this work using vicarious ground targets. Simultaneous overpasses over desert, ocean, Dome C, and RadCalNet sites reveal that the agreement between the four spectrally matching bands is within 3% for the time-period between 2014 and 2020. Also, observed are some long-term drifts in the TOA reflectance time-series from MISR for the red and NIR bands that are

expected to be corrected in a future calibration reprocess. Minor reflectance drifts were also observed in the MISR green band that expected to be addressed in the next L1B reprocess.

Recently, the MODIS Characterization Support Team (MCST) delivered a set of entire mission LUTs for Collection 7 L1B processing. These LUTs include various algorithm enhancements with noticeable changes in Band 9 (443 nm). Minor improvements are also expected for the other bands shown in this comparison. Similar reprocessing efforts on the MISR L1B are also underway and expected to be operational in late 2022. The Terra MODIS instrument's polarization sensitivity at short wavelengths has experienced significant changes on-orbit. The effects due to Earth scene polarization need to be considered for an accurate cross-calibration, particularly for the short wavelength band pairs. Another intercomparison technique involves the use of the Moon as a stable reference to compare the calibration performance of satellite instruments. While MODIS observes the Moon via a roll maneuver on a near-monthly basis, MISR has only viewed the Moon, together with MODIS, twice via a pitch maneuver in its mission, one in 2003 and another in 2017. As MODIS can make frequent lunar observations, these data can be used to monitor detector response changes with time. MISR, however, cannot view the moon during the roll maneuver, and therefore does not have the data to use the Moon for long-term trending. MISR can observe the moon during the pitch maneuver, but this has only been done twice, out of concern for the spacecraft safety. MISR is not a scanning instrument; the nine cameras are fixed onto the instrument optical bench such that they view at along track angles of nadir, $\pm 26.1^\circ$, $\pm 45.6^\circ$, $\pm 60.0^\circ$ and $\pm 70.5^\circ$. During the pitch maneuver the cameras view the moon in turn as the spacecraft flips upside down. These data have been used to validate the relative response of the nine cameras, one to another. Future work involves the comparison of the lunar irradiance measured by the spectrally matching bands of MODIS and MISR normalized by a common reference such as the

USGS ROLO model, but it presents challenges as several factors need to be considered before an accurate cross-comparison of lunar-measured radiances is performed.

Acknowledgements

The MISR datasets were obtained from the NASA Langley Research Center Atmospheric Science Data Center. The RadCalNet data was provided by Dr. Brian Wenny and the authors would also like to thank Drs. Brian Wenny and Kurt Thome for RadCalNet related discussions. The efforts of Michael Bull in processing the MISR RRV data and Marcin Witek for MISR discussions are also appreciated. We would also like to thank Daniel Link of MCST for a technical review of this manuscript. This manuscript is an extension of an SPIE conference proceedings paper (citation below)

Angal, A., C. Bruegge, X. Xiong, and A. Wu, "Intercalibration of the reflective solar bands of MODIS and MISR instruments on the Terra platform", Proc. SPIE - Earth Observing Systems XXVI, vol. 11829, pp. 118291B, 2021.

References

1. J. Butler, and R. A. Barnes, "Calibration Strategy for the Earth Observing System (EOS)-AM1 Platform", IEEE Trans. Geosci. Remote Sens., 36(4), 1056-1061, (1998).
2. W. Barnes, T. S. Pagano, and V. Salomonson, "Prelaunch Characteristics of the Moderate Resolution Imaging Spectroradiometer (MODIS) on EOS-AM1", IEEE Trans. Geosci. Remote Sens., v36 (4), 1088-1100 (1998).
3. X. Xiong, K. Chiang, J. Esposito, B. Guenther, and W. Barnes, "MODIS On-Orbit Calibration and Characterization", Metrologia, 40 (1), 89-92, (2003).

4. D. J. Diner et al., "Multi-angle Imaging SpectroRadiometer (MISR) instrument description and experiment overview," in *IEEE Transactions on Geoscience and Remote Sensing*, 36 (4), 1072-1087, (1998).
5. C. J. Bruegge, N. L. Chrien, R. R. Ando, et al., "Early validation of the Multi-angle Imaging SpectroRadiometer (MISR) radiometric scale," *IEEE Transactions on Geoscience and Remote Sensing* 40(7), 1477–1492 (2002).
6. M. Bouvet, et al. "RadCalNet: A radiometric calibration network for Earth observing imagers operating in the visible to shortwave infrared spectral range." *Remote Sensing* 11 (20), 2401, (2019).
7. J. S. Czapla-Myers, C. A. Coburn, K. J. Thome, B. N. Wenny, and N. J. Anderson, "Directional reflectance studies in support of the Radiometric Calibration Test Site (RadCaTS) at Railroad Valley," *Proc. SPIE*, 10764, 107640Z, (2018).
8. J. Sun, and X. Xiong, "MODIS Polarization Sensitivity Analysis", *IEEE Trans. Geosci. Remote Sens.*, 45, 9, 2875-2885, (2007).
9. G. Thuillier, M. Hersé, T. Foujols, et al., "The Solar Spectral Irradiance from 200 to 2400 nm as Measured by the SOLSPEC Spectrometer from the Atlas and Eureka Missions," *Solar Physics* 214(1), 1–22 (2003).
10. E. V. Smith and D. M. Gottlieb, "Solar flux and its variations," *Space Science Reviews* 16(5), 771–802 (1974).
11. H. Neckel et al., "The solar radiation between 3300 and 12500 Å," *Solar Physics* 90(2), 205–258 (1984).

12. C. J. Bruegge, G. T. Arnold, J. Czapla-Myers, et al., "Vicarious Calibration of eMAS, AirMSPI, and AVIRIS Sensors During FIREX-AQ," *IEEE Transactions on Geoscience and Remote Sensing* (2021).
13. X. Xiong, A. Angal, W. L. Barnes, H. Chen, V. Chiang, X. Geng, Y. Li, K. Twedt, Z. Wang, T. Wilson, et al., "Updates of Moderate Resolution Imaging Spectroradiometer on-orbit calibration uncertainty assessments", *Journal of Applied Remote Sensing*, 12(3), 034001, (2018).
14. X. Xiong, A. Angal, K. A. Twedt, H. Chen, D. Link, X. Geng, E. Aldoretta, and Q. Mu, "MODIS Reflective Solar Bands On-Orbit Calibration and Performance", *IEEE Transactions on Geoscience and Remote Sensing*, 57 (9), 6355-6371, (2019).
15. A. Angal, X. Xiong, and A. Wu, "Monitoring the On-Orbit Calibration of Terra MODIS Reflective Solar Bands Using Simultaneous Terra MISR Observations", *IEEE Transactions on Geoscience and Remote Sensing*, 55 (3), 1648-1659, (2017).
16. B. Scarino et al. "A web-based tool for calculating spectral band difference adjustment factors derived from SCIAMACHY hyperspectral data." *IEEE Transactions on Geoscience and Remote Sensing*, 54(5), 2529-2542, (2016).
17. J. A. Limbacher and R. A. Kahn, "Updated MISR dark water research aerosol retrieval algorithm – Part 1: Coupled 1.1 km ocean surface chlorophyll a retrievals with empirical calibration corrections," *Atmospheric Measurement Techniques* 10(4), 1539–1555 (2017).
18. C. J. Bruegge, et al. "Radiometric stability of the Multi-angle Imaging SpectroRadiometer (MISR) following 15 years on-orbit." *Proc. SPIE*, 9218, (2014).
19. J. Limbacher and R. Kahn, "MISR empirical stray light corrections in high-contrast scenes," *Atmospheric Measurement Techniques* 8(7), 2927–2943 (2015).

20. M. L. Witek, D. J. Diner, M. J. Garay, F. Xu, M. A. Bull, and F. C. Seidel, “Improving MISR AOD retrievals with low-light-level corrections for veiling light” *IEEE Trans. Geosci. Remote Sens.*, 56, 1251–1268, (2018)
21. M. L. Witek, M. J. Garay, D. J. Diner, et al., “New approach to the retrieval of AOD and its uncertainty from MISR observations over dark water,” *Atmospheric Measurement Techniques* 11(1), 429–439 (2018).
22. M. J. Garay, M. L. Witek, R. A. Kahn, et al., “Introducing the 4.4 km spatial resolution Multi-Angle Imaging SpectroRadiometer (MISR) aerosol product ,” *Atmospheric Measurement Techniques* 13(2), 593–628 (2020).
23. A. Angal, X. Geng, X. Xiong, et al., “On-Orbit Calibration of Terra MODIS VIS Bands Using Polarization-Corrected Desert Observations,” *IEEE Transactions on Geoscience and Remote Sensing* 58(8), 5428–5439 (2020).
24. O. M. Coddington, E. C. Richard, D. Harber, et al., “The TSIS-1 Hybrid Solar Reference Spectrum,” *Geophysical Research Letters* 48(12), e2020GL091709 (2021).

Caption List:

Table 1 Summary of key characteristics of the MODIS and MISR RSB

Table 2. MISR Block selection

Table 3. Summary of MODIS/MISR ratios (2014-2020) over multiple targets

Table 4. Summary of MODIS and MISR cross-calibration uncertainty sources

Fig. 1 (a). MODIS and MISR RSR plotted over a sample RVPN Radcalnet profile (b) Radcalnet predicted reflectance ratios

Fig. 2(a). MODIS-MISR TOA reflectance regression for a North African desert overpass from February 2020. (b). MODIS-MISR TOA reflectance regression for the three ground sites using scene pairs from February 2020 for the red-band pair.

Fig. 3. MODIS-MISR TOA reflectance as a function of MODIS frame number (scan angle) from multiple years (a) blue bands (b) green bands (c) red bands (d) NIR bands.

Fig. 4. At-sensor reflectance trending over the North African desert target for the spectrally matching MODIS and MISR bands (plotted in green and red colors, respectively).

Fig. 5. At-sensor reflectance ratios over multiple targets for the spectrally matching MODIS and MISR bands.

Fig. 6. At-sensor reflectance ratios over North Atlantic Ocean for the spectrally matching MODIS ocean bands and MISR bands.

Figure 7 (a) Green, (b) Red, and (c) NIR bands (measured/model of all available RadCalNet matchups). MODIS data is shown in red and MISR in black. Blue band pair not shown here due to saturation observed in MODIS data.